Journal of *Marine Science and Engineering*

MDPI

*Article*

# Modern Techniques for Flood Susceptibility Estimation across the Deltaic Region (Danube Delta) from the Black Sea's Romanian Sector

**Anca Crăciun [1,2], Romulus Costache [2,3], Alina Bărbulescu [3,*], Subodh Chandra Pal [4], Iulia Costache [5] and Cristian Ștefan Dumitriu [6]**

[1] Doctoral School in Ecology, Faculty of Biology, University of Bucharest, 91–95 Splaiul Independentei, 050095 Bucharest, Romania
[2] Danube Delta National Institute for Research and Development, 165 Babadag Street, 820112 Tulcea, Romania
[3] Department of Civil Engineering, Transilvania University of Brasov, 5, Turnului Street, 500152 Brasov, Romania
[4] Department of Geography, The University of Burdwan, Bardhaman 713104, West Bengal, India
[5] Faculty of Geography, University of Bucharest, 010041 Bucharest, Romania
[6] Doctoral School, Technical University of Civil Engineering, Bucharest, 124 Lacul Tei Bd., 020396 Bucharest, Romania
* Correspondence: alina.barbulescu@unitbv.ro

**Abstract:** Floods have become more and more severe and frequent with global climate change. The present study focuses on the Black Sea's immediate riparian area over which the Danube Delta extends. Due to the accelerated increase in the severity of floods, the vulnerability of the deltaic areas is augmenting. Therefore, it is very important to adopt measures to mitigate the negative effects of these phenomena. The basis of the measures to limit the negative effects is the activity of identifying areas prone to flooding. Thus, this research paper presents a methodology for estimating flood susceptibility using the Analytical Hierarchy Process (AHP) and Fuzzy-Analytical Hierarchy Process (FAHP) models. To determine the susceptibility to these natural risk phenomena, the following eight flood predictors were taken into account: slope, elevation, altitude above channel, land use, hydrological soil group, lithology distance from the river, and distance from water bodies. Furthermore, the weights that each flood predictor has in terms of determining flood susceptibility were determined through the previously mentioned models. The results revealed that the slope is the most important predictor, followed by elevation, distance from the river, and land use. These weights were used in the GIS environment to evaluate the susceptibility to floods from a spatial point of view. The areas with a high/very high value for these phenomena occupy over 70% of the surface of the Danube Delta.

**Keywords:** Danube Delta; flood susceptibility; Fuzzy-Analytical Hierarchy Process; geographic information system



**Citation:** Crăciun, A.; Costache, R.; Bărbulescu, A.; Pal, S.C.; Costache, I.; Dumitriu, C.Ș. Modern Techniques for Flood Susceptibility Estimation across the Deltaic Region (Danube Delta) from the Black Sea's Romanian Sector. *J. Mar. Sci. Eng.* **2022**, *10*, 1149. https://doi.org/10.3390/jmse10081149

Academic Editor: Wei-Bo Chen

Received: 1 August 2022
Accepted: 18 August 2022
Published: 19 August 2022



## 1. Introduction

Due to their impact on dynamic hydraulic hazards that cause widespread damage on a variety of scales, floods have caused enormous socioeconomic losses and environmental devastation around the world [1–4]. It is a global challenge to reduce the risk of floods and manage water resources under changing environmental conditions. In addition to their complexity, floods are prone to varying damages depending on the geography in which they occur. For this reason, it is important to use advanced methods and tools to identify the areas susceptible to flooding.

Floods have also been intensifying and becoming more powerful due to climate changes, causing severe damage to property and human lives [5]. There has been an increase in the global temperature and the intensity and frequency of rainfall due to

changing climate conditions. Due to these climatic changes, there has been an augmentation of peak discharges, runoff, and flood events. Instead, according to the Intergovernmental Panel on Climate Change (IPCC), flood impacts will also vary depending on the climate scenarios' variability and the environment's state in the affected regions [6]. Several studies have demonstrated that climate variability can potentially increase the vulnerability of the natural and human ecosystems to events such as floods, droughts, cyclones, heat waves, and wildfires [7–10]. As a result of this level of warming, the runoff trend for some of the countries in the north latitudinal zone, such as Romania, East Africa, Northeast Europe, Hungary, China, and the Scandinavian countries, will be significantly higher as well. Around 2.3 billion people worldwide have been affected by flooding, which accounts for about 47% of all weather-related disasters [11].

In most parts of the world, deltas and flood plains are sensitive to the erosion of river banks as well as floods from rivers. In order to estimate floods from rivers, hydraulic modelling and flood susceptibility indices are widely used across the world. The nature and trend of rainfall, river discharge, and frequency of cyclonic events over the past few years have radically changed due to changes in the nature and trend of rainfall. As a result, we must study environmental issues and manage complex risks to maintain a healthy environment. It should be mentioned that river deltas are regions that are highly vulnerable to the effects of environmental changes and are extremely vulnerable to natural disasters, especially floods, due to their high vulnerability to climate change. The delta floodplains are extremely important to maintain the dynamics of the entire natural system. Due to this reason, it is very important to study the natural hazards that can affect the natural system of deltaic regions and coastal regions and to highlight especially the surfaces that are prone to these natural disasters. Floods are essential to both alluvial processes in deltaic lakes as well as to supplying water to them [12]. Flooding frequency is important because it flushes the water from the deltaic lake system, ensuring that both the terrestrial and aquatic ecosystems can evolve normally [13]. For human communities, however, floods can be regarded as a potential source of harm, causing physical and psychological distress, as well as causing material damage. An accurate and appropriate susceptibility analysis can help decrease the severity of these consequences. Scientists and government officials must produce accurate flood models to help them make informed decisions. Literature has used a variety of hydrological approaches over the years to understand the hydrological process [14]. Several traditional hydrological techniques are incapable of comprehensively analyzing rivers and inundation areas, such as physical model-based rainfall-runoff analysis and data-driven analysis. A considerable contribution has been made to flood modeling and prediction through remote sensing techniques (RS) and geographic information systems (GIS) [15]. The RS and GIS techniques provide a variety of data sources, a high level of data quality, tracking capacity during the day and the night [16,17], and the capability to analyze data quickly.

Several multi-criteria decisions making (MCDM) models have been successfully combined with geographic information systems (GIS) for flood susceptibility mapping, especially the Analytic Hierarchy Process (AHP) and Analytic Network Process (ANP) [18]. To make an optimal decision, AHP assists in quantifying the relative importance of flood causative criteria using the user's decision parameters, and it is one of the most widely used methods of MCDM for identifying flood-prone areas [19]. The main disadvantage of the AHP, however, is that the results are subject to uncertainty and imprecision when compared due to inconsistencies or biases in the pairwise comparison. To address this limitation, a fuzzy algorithm has been integrated into medium-complexity decision-making models (MCDMs) [20]. In this model, the criterion weighting and alternative selection are made more accurate to modify the original AHP for more accurate weighting and alternative selection. The high precision of fuzzy AHP has been used in different geohazard scenarios for GIS modeling because of its compatibility with GIS. Therefore, the present paper aims to develop an accurate flood susceptibility mapping procedure using the Fuzzy-AHP model

for the Danube Delta region. Eight flood predictors are considered and integrated into the GIS and Fuzzy-AHP model.

## 2. Study Area

The present research study is focused on the Danube Delta from Romania (Figure 1). With an area of 5640 km$^2$, the Danube Delta is one of the largest ecosystems of the humid zones in Europe, taking up the most significant portion of the area. In terms of liquid and solid parameters, it measures the state of the environment at both a local and regional level, but it also ensures a steady water supply at both the local and regional levels so that the local economy and community can thrive.

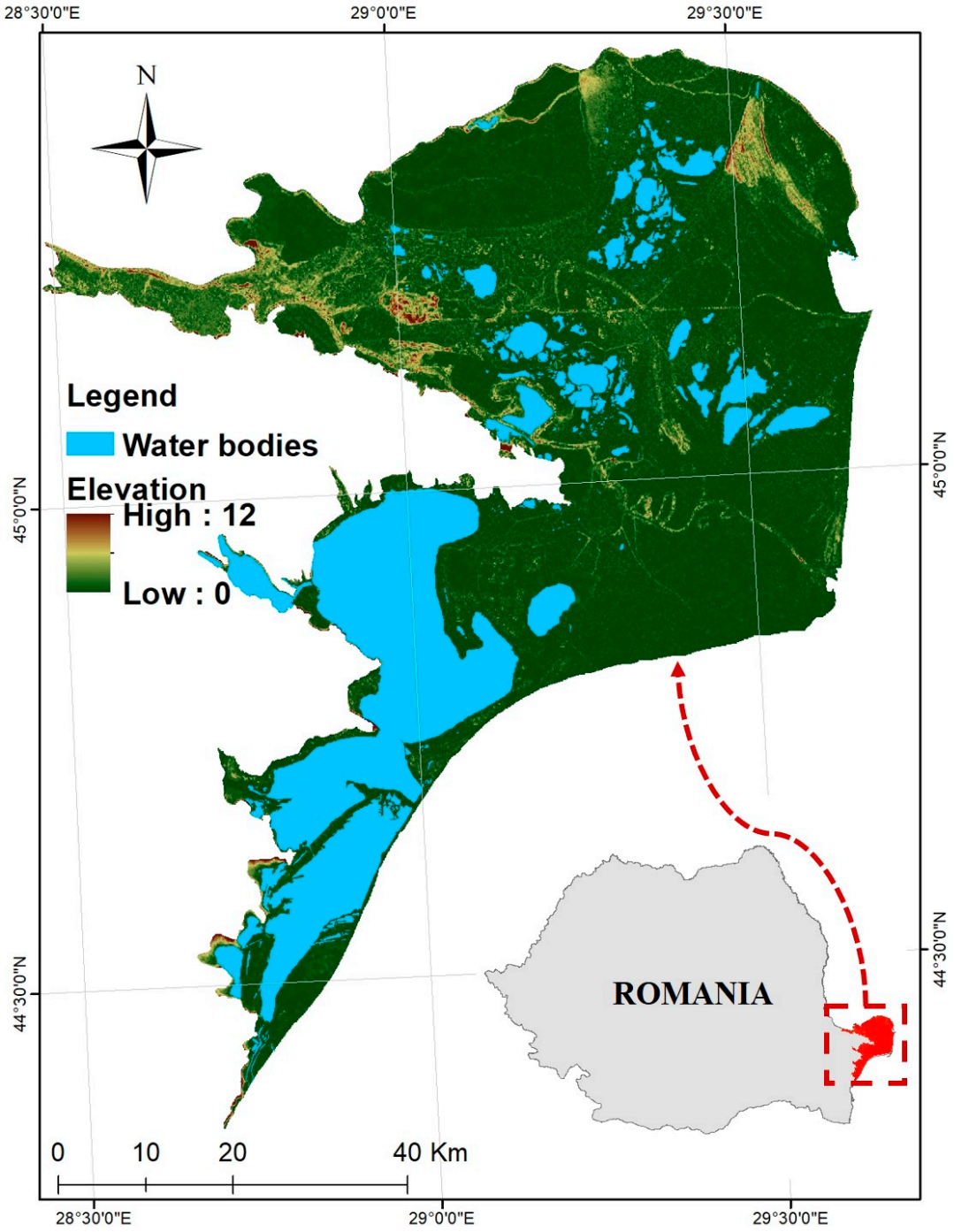


**Figure 1.** Location of the study area.

In the last 5200 years, the Black Sea's level has been stabilizing since the Black Sea's region was carved into a gulf by the delta, running between Bugeac Plain and the Dobrogea Plateau, at which point the delta is enclosed within a gulf. A morphological analysis of the area associates the Danube Delta with that of a developing alluvial plain, which can be defined as a region with reduced hypsometry (with no greater than 13 m difference in elevation in the emergent area and a difference of 64 m between the height of the Letea fluvial-maritime levee and the depth of the Tulcea Branch). As the average and maximum annual flows increased between 1945 and 2007, as well as did the average monthly distribution of maximum water flows between March and June, the average monthly distribution of maximum annual flows had a general tendency to rise relatively. Several major floods occurred along the Danube in 1895, 1926, 1942, 1970, 1975, 1981, 1988, and 2006 [21].

## 3. Data

Choosing the geographical factors that are most relevant to describing a flood's impact is one of the most important factors in determining flood susceptibility values in a given area. It is important to note that this is another step towards arriving at an accurate estimate of flood susceptibility values across a given spatial area. The following rows provide descriptions of the eight flood predictors used in this analysis. Three predictors are derived from the Digital Elevation Model: slope angle, elevation, and altitude above the channel. The Digital Elevation Model was extracted from the Shuttle Radar Topographic Mission (SRTM) 30 m database [22]. The other five flood predictors were achieved from vectorial databases: distance from rivers and channels, land use, lithology, hydrological soil groups, and distance from water bodies.

The slope angle plays an important role not only in terms of flood severity but also in the amount of water that accumulates due to runoff processes [23]. In light of this phenomenon, slopes with a high precipitation amount determine the flow of water to low-sloped areas, where water tends to accumulate since slopes with a high amount of precipitation cause a high amount of rain to fall. In the present research, the slope classes are the following: 0–1°, 1.1–2°, 2.1–3°, 3.1–4°, and >4° (Figure 2a).

The elevation of a particular region plays a significant role in determining the likelihood of flooding in a specific area as it is a morphometric factor that promotes a specific geographical feature [24]. The elevation was split into eight classes: 0–1 m, 1.1–2 m, 2.1–3 m, 3.1–4 m, 4–5 m, 5–6 m, 7–8 m, and >8 m (Figure 2b).

Floods are more likely to occur in areas that are less than 50 m from rivers because of the proximity to rivers [25]. The distance from rivers and channels factor was derived with the help of Euclidean Distance procedure implemented in ArcGIS 10.5 (Esri, Bucharest, Romania) software. In order to create the distance from the river map, the following eight classes were established: 0–50 m, 50.1–100 m, 100.1–150 m, 150.1–200 m, 200.1–400 m, 400.1–700 m, 700.1–1000 m, and >1000 m (Figure 2c).

Due to the different values of Manning roughness coefficients, land use is one of the most important predictors of floods due to its influence on the velocity of surface runoff. The land-use map of the Danube Delta was derived using the Corine Land Cover database. According to this database, eleven land use categories could be determined in the Danube Delta region (Figure 2d).

The altitude above channel refers to the altitude difference between the closest channel network and the surrounding region [26]. The regions which are characterized by a low difference in terms of altitude will have a high exposure to flood occurrence. The altitude above the channel was split into eight classes: 0–1 m, 1.1–2 m, 2.1–3 m, 3.1–4 m, 4–5 m, 5–6 m, 7–8 m, and >8 m (Figure 3a).

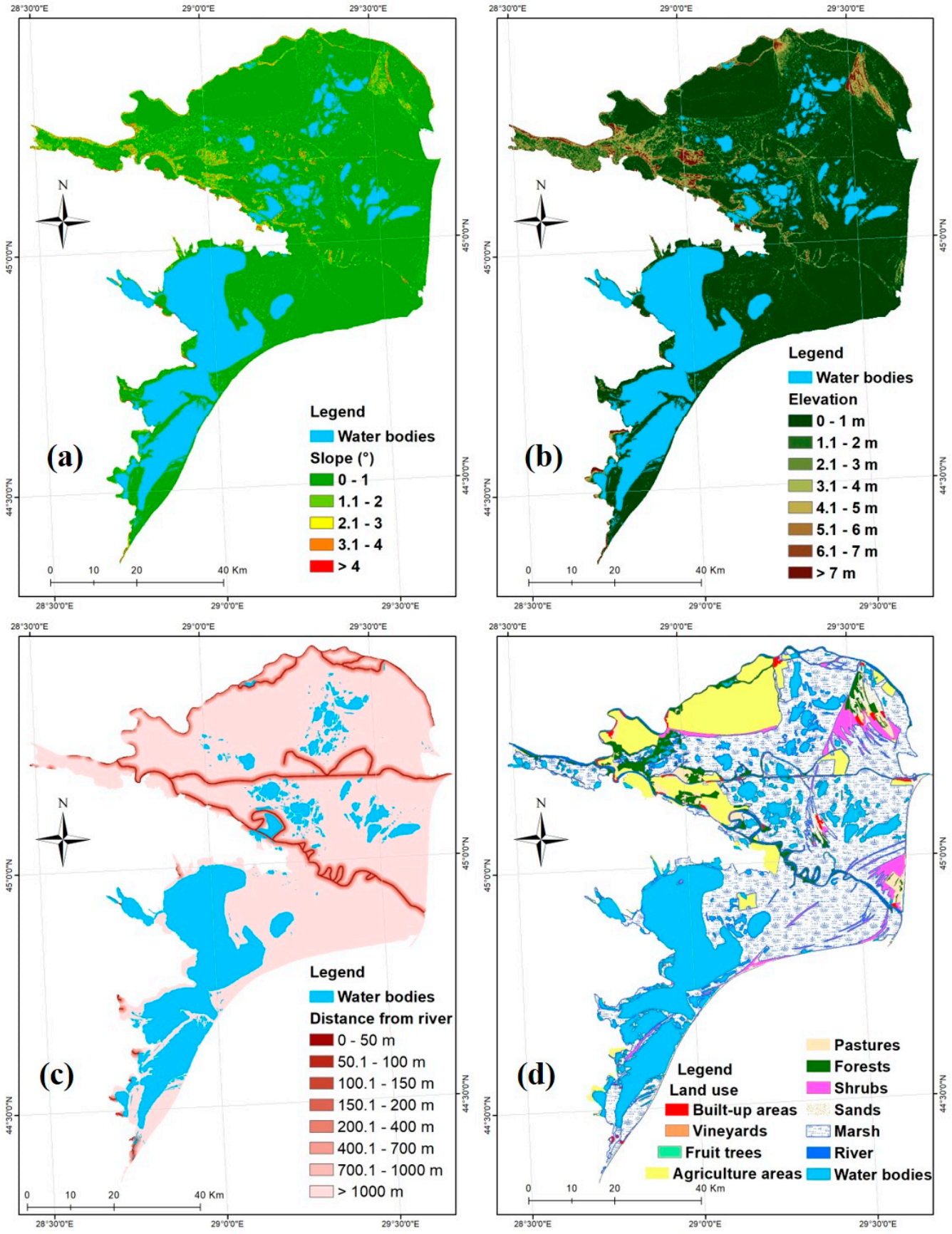


**Figure 2.** Flood predictors. ((**a**) Slope, (**b**) elevation, (**c**) distance from water, (**d**) land use).

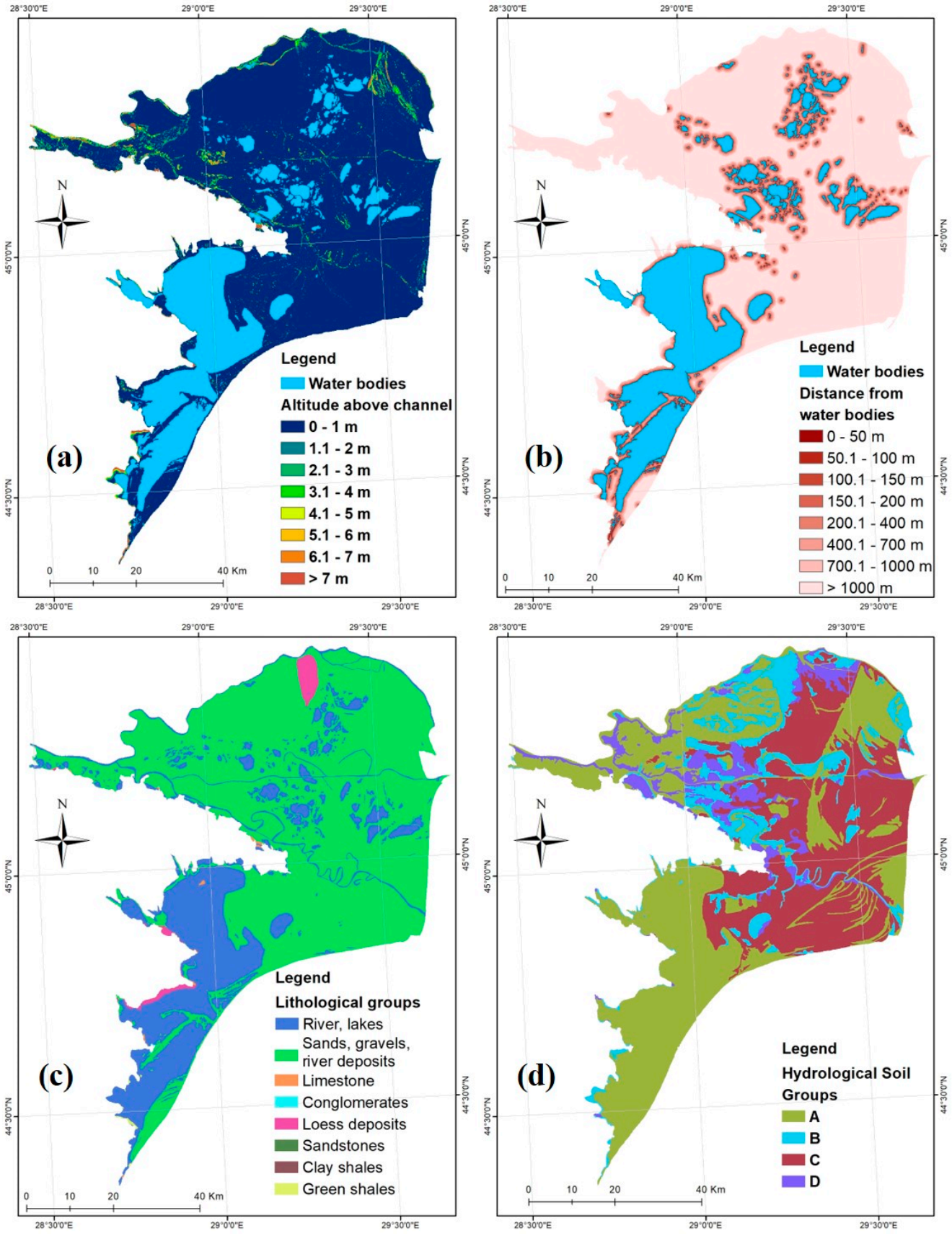


**Figure 3.** Flood predictors ((**a**) Altitude above channel, (**b**) distance from water bodies; (**c**) lithological groups; (**d**) hydrological Soil Groups).

In the Danube Delta, the water bodies are present in large areas. Any increase in the water level of these water bodies represents a dangerous phenomenon for the regions within proximity. The distance from water bodies factor was also derived using the Euclidean Distance procedure. In order to create the distance from water bodies, the following eight classes were established: 0–50 m, 50.1–100 m, 100.1–150 m, 150.1–200 m, 200.1–400 m, 400.1–700 m, 700.1–1000 m, and >1000 m (Figure 3b).

The lithology significantly influences the shape and morphology of river valleys, just as it controls how water infiltrates [27,28]. Lithological categories of the study zone were obtained from the Geological Map of Romania, 1:200.000. Eight lithological categories were selected for the present research according to Figure 3c.

Water infiltration velocity is also influenced by the type of soil group and can drastically affect the amount of water that accumulates at the ground surface [29]. Romanian Soil Map in Digital format, 1:200.000, was used as a data source for the present study. According to Figure 3d, all four hydrological groups are present in the Danube Delta.

## 4. Methods

The Fuzzy-Analytical Hierarchical Process (FAHP) aims to improve the quality of the analysis through the combination of fuzzy set theory with the AHP algorithm, which aims to reduce subjectivity in calculating the judge's weights and increase the rigor of the analysis. Using the FAHP model, we calculate the weights for each flood conditioning factor within the equation of flood susceptibility. The main aspects of fuzzy set theory and the AHP algorithm will be presented in the following section along with the combination of these two models as a whole.

As a semi-quantitative algorithm, the Analytical Hierarchy Process (AHP) is frequently used to assess an area's susceptibility to natural hazards. Using the AHP model, the main objective is to compute the weights of different criterion map layers based on the expert knowledge gathered during constructing the pairwise comparison matrix. To solve the hierarchical fuzzy problems arising from a hierarchical structure, FAHP, an extension of the AHP algorithm that is fuzzy was used in place of the conventional AHP algorithm, since the conventional AHP algorithm cannot reflect the human thinking style. As part of the FAHP model, it is possible to determine the weights of the various criteria based on the following two steps:

(i) During the construction of the pairwise comparison matrices, all flood conditioning factors were taken into account. A linguistic term was assigned to the pairwise comparison so that we would be able to determine which element/criteria is more important to the individual. The following linguistic terms were assigned:

$$A' = \begin{bmatrix} 1' & a'_{12} & \cdots & a'_{1n} \\ a'_{21} & 1' & \cdots & a'_{1n} \\ \vdots & \vdots & \ddots & \vdots \\ a'_{n1} & a'_{n2} & \cdots & 1' \end{bmatrix} = \begin{bmatrix} 1' & a'_{12} & \cdots & a'_{1n} \\ 1/a'_{21} & 1' & \cdots & a'_{1n} \\ \vdots & \vdots & \ddots & \vdots \\ 1/a'_{n1} & 1/a'_{n2} & \cdots & 1' \end{bmatrix} \quad (1)$$

where $a'_{ij}$ shows a pair of criteria $i$ and $j$.

Let $1'$ be (1, 1, 1), when $i = j$, if $1'$, $2'$, $3'$, $4'$, $5'$, $6'$, $7'$, $8'$, and $9'$ measure that variable $i$ which has a higher relative importance in comparison with variable $j$, whereas $1/1'$, $1/2'$, $1/3'$, $1/4'$, $1/5'$, $1/6'$, $1/7'$, $1/8'$, and $1/9'$ measure that variable $j$ which is relatively more important.

(ii) Through the Buckley method, the weight and fuzzy geometric mean of each criterion were calculated by:

$$r'_i = \left(a'_{i1} \otimes a'_{i2} \otimes \ldots \otimes a'_{in}\right)^{1/n}, \quad (2)$$

and then

$$w'_i = r'_i \otimes (r'_1 \otimes \ldots \otimes r'_n)^{-1} \quad (3)$$

where $a'_{in}$ represents the value of fuzzy comparison among the pair criterion $n$ and criterion $i$, $r'_1$ represents the value of geometric mean associated to the fuzzy comparison values for criterion $i$ compared to each of the other criteria, and $w'_i$ is the fuzzy weighting of the $i$th criterion, which can be also represented by a TFN; $w'_i = (lw_i,\ mw_i,\ uw_i)$, where $lw_i$, $mw_i$, and $uw_i$ are the lower, middle, and upper values, respectively, of the fuzzy weighting of the $i$th criterion.

Using the extent analysis algorithm, it was possible to determine the final values of the corresponding flood predictor weights that would be used in the flood prediction model. In order to construct a fuzzy triangular comparison matrix form at the beginning of this algorithm, we have to construct the following:

$$A' = \left(a'_{ij}\right)_{nxn} = \begin{bmatrix} (1,1,1) & (l_{12},\ m_{12}, u_{12}) & \cdots & (l_{1n},\ m_{1n}, u_{1n}) \\ (l_{21},\ m_{21}, u_{21}) & (1,1,1) & \cdots & (l_{2n},\ m_{2n}, u_{2n}) \\ \vdots & \vdots & \ddots & \vdots \\ (l_{n1},\ m_{n1}, u_{n1}) & (l_{n2},\ m_{n2}, u_{n2}) & \cdots & (1,1,1) \end{bmatrix} \tag{4}$$

where $a'_{ij} = (l_{ij},\ m_{ij}, u_{ij}) = a'^{-1}_{ij} = (1/l_{ij},\ 1/m_{ij}, 1/u_{ij})$ for $i, j = 1, \ldots, n$ and $i \neq j$.

The extent analysis method and the priority vector of the triangular matrix will be calculated. Thus, in a first stage, the fuzzy arithmetic function will be employed to sum up each row of matrix $A'$:

$$RS_i = \sum_{j=1}^{n} a'_{ij} = \left(\sum_{j=1}^{n} l_{ij}, \sum_{j=1}^{n} m_{ij}, \sum_{j=1}^{n} u_{ij}\right),\ \ i = 1, \ldots,\ n \tag{5}$$

Through the normalization of the above relation, the value of the fuzzy synthetic extent in terms of the $i$th object can be obtained as follows:

$$S'_i = \sum_{j}^{n} a'_{ij} \bigotimes \left[\sum_{k=1}^{n}\sum_{j=1}^{n} a'_{kj}\right]^{-1} = \left(\frac{\sum_{j=1}^{n} l_{ij}}{\sum_{k=1}^{n}\sum_{j=1}^{n} u_{kj}}, \frac{\sum_{j=1}^{n} m_{ij}}{\sum_{k=1}^{n}\sum_{j=1}^{n} m_{kj}}, \frac{\sum_{j=1}^{n} u_{ij}}{\sum_{k=1}^{n}\sum_{j=1}^{n} l_{kj}}\right),\ i = 1, \ldots,\ n. \tag{6}$$

The computation of the degree of possibility of $S'_i \geq S'_j$ (Figure 4) represents the third step and is achieved through the following formula:

$$V(S'_i \geq S'_j) = \begin{cases} 1, if\ m_i \geq m_j, \\ \dfrac{u_i - l_j}{(u_i - m_i) + (m_j - l_j)}, l_j \leq\ u_i, \quad i, j = 1,\ \ldots,\ n; j \neq i \\ 0, \text{others} \end{cases} \tag{7}$$

where $S'_i = (l, m_i, u_i)$ and $S'_j = \left(l_j, m_j, u_j\right)$.

Considering that:

$$w'(a_i) = \min\left\{V(S'_i \geq S'_k)\right\},\ k = 1,\ 2,\ \ldots.,\ \text{n};\ k\ \neq\ i, \tag{8}$$

the value of weight vector will be calculated as:

$$w'(a_i) = \left[w'(a_i),\ w'(a_i),\ \ldots,\ w'(a_i)\right]^{\ T}, \tag{9}$$

where $A_i$ ($i = 1, 2, \ldots, n$) are $n$ elements.

After the normalization process, the weight vectors can be obtained using the following relation:

$$w(a_i) = \left[w(a_1),\ w(a_2),\ \ldots,\ w(a_n)\right]^{\ T}, \tag{10}$$

where $w$ is a non-fuzzy number.

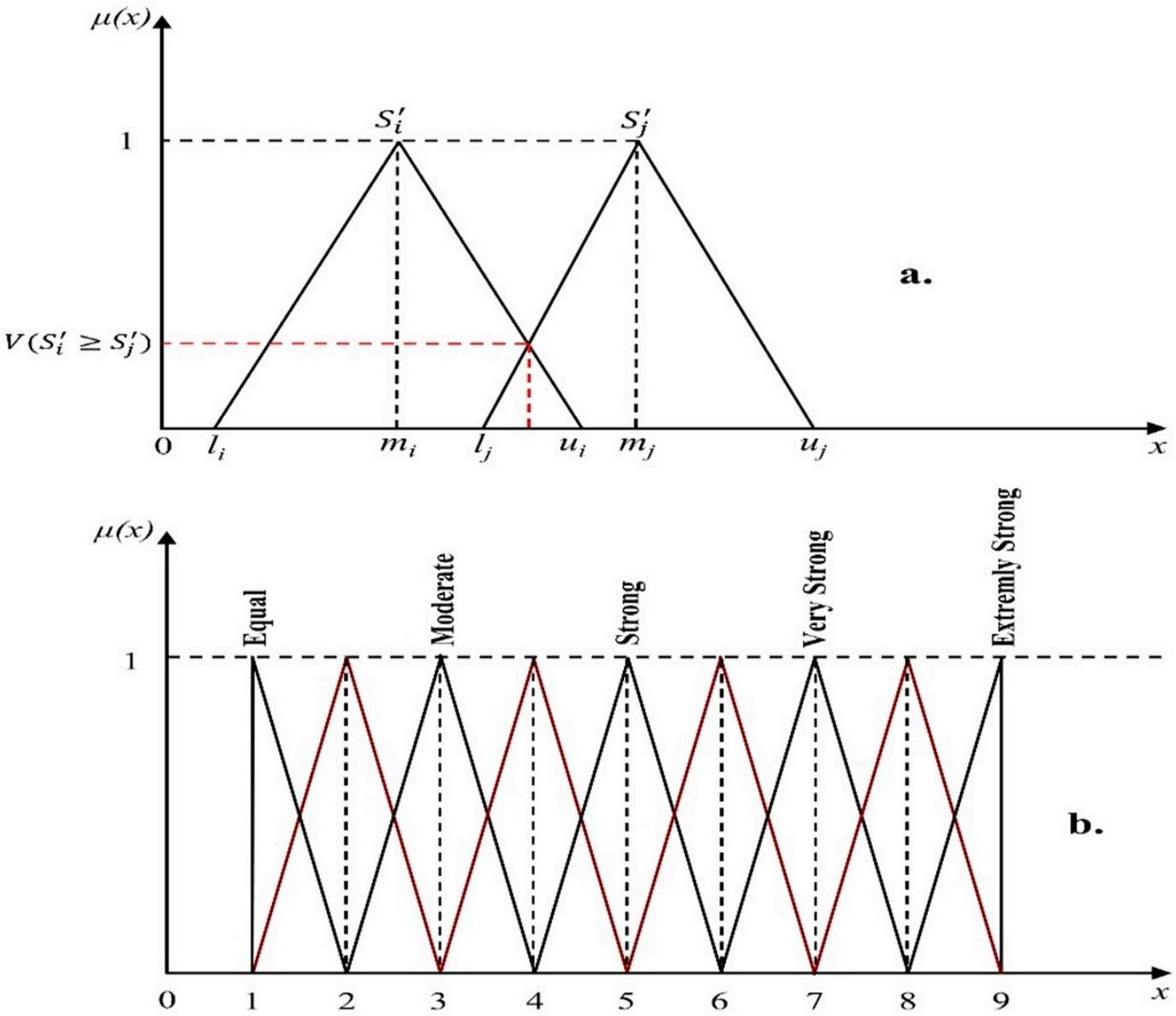


**Figure 4.** (**a**) The degree of possibility of $S_i' \geq S_j'$; (**b**) Triangular fuzzy number corresponding to linguistic variables according to the level of preference.

In order to develop the flood potential index using the FAHP stand-alone model, in the first step of the process, an Analytic Hierarchy Process was used to calculate the weights of each of the factor classes and categories within the FAHP stand-alone model. We were able to achieve this in part by utilizing eight comparison matrices that were generated in the Microsoft Excel 2013 software in order to calculate the AHP weights. Several scientific papers have described the entire procedure of the AHP algorithm [30–32]. It was necessary to assign weights to each class of factors based on the AHP weights, with ArcGIS 10.5. A second step consisted of building a Fuzzy-Analytical Hierarchy Process evaluation matrix for each factor class/category in Microsoft Excel 2013, which was then used to calculate the weights of each flood condition factor in ArcGIS 10.5.

The final step in computing the flood potential index through the FAHP model was multiplying the flood conditioning factors raster in ArcGIS 10.5 with the weights calculated from the AHP model, and the weights generated by the AHP model were then applied to the raster.

Figure 5 presents the workflow implemented in this study.

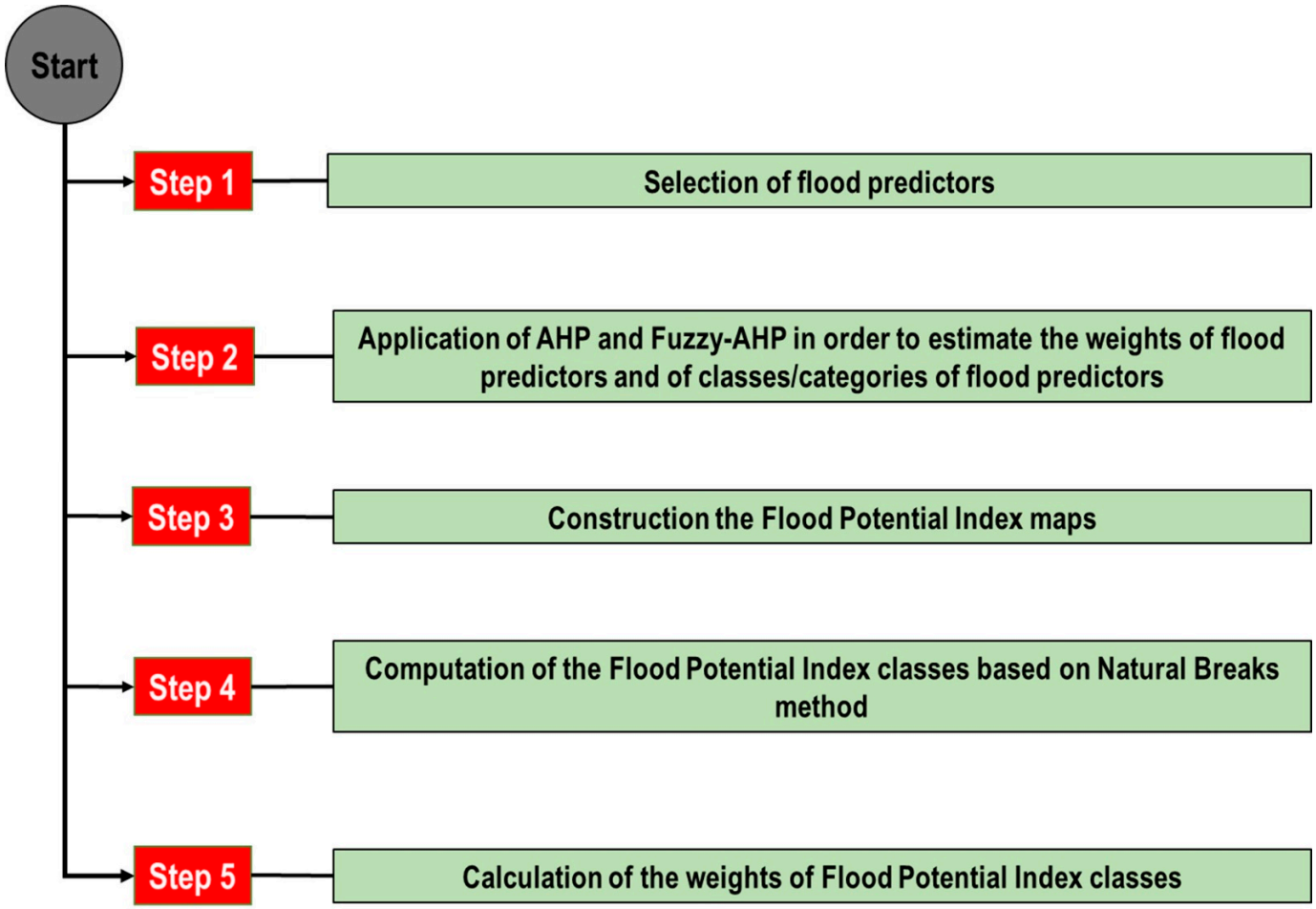


**Figure 5.** Flowchart of the methodology.

## 5. Results

### *5.1. AHP Method*

There are a number of possible combinations between the geographical factors that affect flood occurrences and their classes and categories, which can be found in Table 1. Each factor or class/category was compared with the others by assigning a dominant relative value. These values were assigned after consulting the specialized literature. Their weights are also included in Table 1.

**Table 1.** AHP comparison matrix.

| Factors/Classes Categories | Pairwise Comparison | | | | | | | | AHP Weights |
|---|---|---|---|---|---|---|---|---|---|
| | [1] | [2] | [3] | [4] | [5] | [6] | [7] | [8] | |
| Factors | | | | | | | | | |
| [1] Slope | 1 | 2 | 2 | 3 | 5 | 6 | 7 | 9 | 0.288 |
| [2] Elevation | 1/2 | 1 | 2 | 3 | 5 | 6 | 7 | 9 | 0.239 |
| [3] Distance from river | 1/2 | 1/2 | 1 | 2 | 4 | 5 | 6 | 9 | 0.177 |
| [4] Land use | 1/3 | 1/3 | 1/2 | 1 | 3 | 4 | 5 | 8 | 0.124 |
| [5] Altitude above channel | 1/5 | 1/5 | 1/4 | 1/3 | 1 | 2 | 3 | 7 | 0.068 |
| [6] Distance from water bodies | 1/6 | 1/6 | 1/5 | 1/4 | 1/2 | 1 | 2 | 6 | 0.049 |
| [7] Lithology | 1/7 | 1/7 | 1/6 | 1/5 | 1/3 | 1/2 | 1 | 6 | 0.038 |
| [8] Hydrological Soil Groups | 1/9 | 1/9 | 1/9 | 1/8 | 1/7 | 1/6 | 1/6 | 1 | 0.016 |

**Table 1.** *Cont.*

| Factors/Classes Categories | Pairwise Comparison | | | | | | | | AHP Weights |
|---|---|---|---|---|---|---|---|---|---|
| **Class/categories** | | | | | | | | | |
| Slope (°) | | | | | | | | | |
| [1] 0–1 | 1 | 4 | 6 | 7 | 9 | | | | 0.546 |
| [2] 1–2 | 1/4 | 1 | 3 | 4 | 6 | | | | 0.229 |
| [3] 2–3 | 1/6 | 1/3 | 1 | 2 | 4 | | | | 0.113 |
| [4] 3–4 | 1/7 | 1/4 | 1/2 | 1 | 3 | | | | 0.075 |
| [5] >4 | 1/9 | 1/6 | 1/4 | 1/3 | 1 | | | | 0.037 |
| **Altitude (m)** | | | | | | | | | |
| [1] 0–1 | 1 | 2 | 3 | 4 | 5 | 6 | 7 | 8 | 0.327 |
| [2] 1–2 | 1/2 | 1 | 2 | 3 | 4 | 5 | 6 | 7 | 0.227 |
| [3] 2–3 | 1/3 | 1/2 | 1 | 2 | 3 | 4 | 5 | 6 | 0.157 |
| [4] 3–4 | 1/4 | 1/3 | 1/2 | 1 | 2 | 3 | 4 | 5 | 0.108 |
| [5] 4–5 | 1/5 | 1/4 | 1/3 | 1/2 | 1 | 2 | 3 | 4 | 0.073 |
| [6] 4–6 | 1/6 | 1/5 | 1/4 | 1/3 | 1/2 | 1 | 2 | 3 | 0.050 |
| [7] 6–7 | 1/7 | 1/6 | 1/5 | 1/4 | 1/3 | 1/2 | 1 | 2 | 0.034 |
| [8] >7 | 1/8 | 1/7 | 1/6 | 1/5 | 1/4 | 1/3 | 1/2 | 1 | 0.024 |
| **Distance from the river (m)** | | | | | | | | | |
| [1] 0–50 | 1 | 2 | 3 | 4 | 5 | 6 | 7 | 9 | 0.323 |
| [2] 50–100 | 1/2 | 1 | 2 | 3 | 4 | 5 | 6 | 7 | 0.221 |
| [3] 100–150 | 1/3 | 1/2 | 1 | 2 | 3 | 4 | 5 | 6 | 0.152 |
| [4] 150–200 | 1/4 | 1/3 | 1/2 | 1 | 2 | 3 | 4 | 5 | 0.104 |
| [5] 200–400 | 1/5 | 1/4 | 1/3 | 1/2 | 1 | 3 | 3 | 3 | 0.073 |
| [6] 400–700 | 1/6 | 1/5 | 1/4 | 1/3 | 1/3 | 1 | 4 | 6 | 0.063 |
| [7] 700–1000 | 1/7 | 1/6 | 1/5 | 1/4 | 1/3 | 1/4 | 1 | 6 | 0.043 |
| [8] >1000 | 1/9 | 1/7 | 1/6 | 1/5 | 1/3 | 1/6 | 1/6 | 1 | 0.021 |
| **Land use** | | | | | | | | | |
| [1] Forests, sands | 1 | 1/3 | 1/5 | 1/7 | 1/9 | | | | 0.035 |
| [2] Vineyards, fruit trees, shrubs | 3 | 1 | 1/3 | 1/5 | 1/7 | | | | 0.069 |
| [3] Agriculture areas | 5 | 3 | 1 | 1/3 | 1/5 | | | | 0.136 |
| [4] Pastures | 7 | 5 | 3 | 1 | 1/2 | | | | 0.286 |
| [5] Built-up areas, marsh, river, water bodies | 9 | 7 | 5 | 2 | 1 | | | | 0.474 |
| **Altitude above channel (m)** | | | | | | | | | |
| [1] 0–1 | 1 | 2 | 3 | 4 | 5 | 6 | 7 | 8 | 0.327 |
| [2] 1–2 | 1/2 | 1 | 2 | 3 | 4 | 5 | 6 | 7 | 0.227 |
| [3] 2–3 | 1/3 | 1/2 | 1 | 2 | 3 | 4 | 5 | 6 | 0.157 |
| [4] 3–4 | 1/4 | 1/3 | 1/2 | 1 | 2 | 3 | 4 | 5 | 0.108 |
| [5] 4–5 | 1/5 | 1/4 | 1/3 | 1/2 | 1 | 2 | 3 | 4 | 0.073 |
| [6] 4–6 | 1/6 | 1/5 | 1/4 | 1/3 | 1/2 | 1 | 2 | 3 | 0.050 |
| [7] 6–7 | 1/7 | 1/6 | 1/5 | 1/4 | 1/3 | 1/2 | 1 | 2 | 0.034 |
| [8] >7 | 1/8 | 1/7 | 1/6 | 1/5 | 1/4 | 1/3 | 1/2 | 1 | 0.024 |
| **Distance from water bodies (m)** | | | | | | | | | |
| [1] 0–50 | 1 | 2 | 3 | 4 | 5 | 6 | 8 | 9 | 0.324 |
| [2] 50–100 | 1/2 | 1 | 2 | 3 | 4 | 5 | 7 | 8 | 0.225 |
| [3] 100–150 | 1/3 | 1/2 | 1 | 2 | 3 | 4 | 6 | 7 | 0.156 |
| [4] 150–200 | 1/4 | 1/3 | 1/2 | 1 | 2 | 4 | 5 | 6 | 0.113 |
| [5] 200–400 | 1/5 | 1/4 | 1/3 | 1/2 | 1 | 2 | 3 | 4 | 0.069 |
| [6] 400–700 | 1/6 | 1/5 | 1/4 | 1/4 | 1/2 | 1 | 2 | 6 | 0.053 |
| [7] 700–1000 | 1/8 | 1/7 | 1/6 | 1/5 | 1/3 | 1/2 | 1 | 6 | 0.040 |
| [8] >1000 | 1/9 | 1/8 | 1/7 | 1/6 | 1/4 | 1/6 | 1/6 | 1 | 0.019 |

**Table 1.** *Cont.*

| Factors/Classes Categories | Pairwise Comparison | | | | | AHP Weights |
|---|---|---|---|---|---|---|
| **Lithology** | | | | | | |
| [1] Sands, gravels, river deposits | 1 | 1/2 | 1/4 | 1/6 | 1/9 | 0.043 |
| [2] Loess deposits | 2 | 1 | 1/2 | 1/3 | 1/4 | 0.090 |
| [3] Limestone, conglomerates | 4 | 2 | 1 | 1/2 | 1/5 | 0.142 |
| [4] Clay shale, green shale | 6 | 3 | 2 | 1 | 1/2 | 0.256 |
| [5] Sandstone | 9 | 4 | 5 | 2 | 1 | 0.469 |
| Hydrological Soil Groups | | | | | | |
| [1] A | 1 | 3/4 | 1/2 | 1/5 | | 0.108 |
| [2] B | 4/3 | 1 | 3/4 | 1/3 | | 0.157 |
| [3] C | 2 | 4/3 | 1 | 1/3 | | 0.201 |
| [4] D | 5 | 3 | 3 | 1 | | 0.534 |

It can be seen that slope (0.288) is the factor that, from the experts' perspective, has the most significant influence on the potential for the formation and manifestation of floods, followed in order by elevation (0.239), distance from the river (0.177), land use (0.124), altitude above channel (0.068), distance from water bodies (0.049), lithology (0.038), and hydrological Soil Groups (0.016).

From the viewpoint of the factors' classes/categories weights, the highest value was obtained by a class of slopes below 1° (0.546), followed by soil hydrological group D (0.534), built-up areas, marsh, river, water bodies (0.474), sandstone (0.469), areas at a distance from channels below 50 m (0.362), and altitudes below 1 m (0.327) (Table 1).

As mentioned in the Methods section, the comparison matrices' quality was assessed by Consistency Rate (CR) values. According to Table 2, the CR values assigned to all nine comparison matrices are lower than 0.1, which shows a good quality of the analysis. The values of the other parameters of the AHP model were also included in Table 2.

**Table 2.** Properties of AHP pairwise comparison matrices.

| Factors | No. of Factors/Classes | $\lambda_{max}$ | CI | RI | CR |
|---|---|---|---|---|---|
| All factors | 8 | 8.067 | 0.010 | 1.41 | 0.007 |
| Slope | 5 | 5.223 | 0.056 | 1.12 | 0.050 |
| Elevation | 8 | 8.048 | 0.007 | 1.41 | 0.005 |
| Distance from river | 8 | 8.351 | 0.050 | 1.41 | 0.036 |
| Land use | 5 | 5.223 | 0.056 | 1.12 | 0.050 |
| Altitude above channel | 8 | 8.048 | 0.007 | 1.41 | 0.005 |
| Distance from water bodies | 8 | 8.351 | 0.050 | 1.41 | 0.036 |
| Lithology | 5 | 5.223 | 0.056 | 1.12 | 0.050 |
| Hydrological Soil Groups | 4 | 4.011 | 0.004 | 0.9 | 0.004 |

The weights assigned to the factor classes/categories were used to derive new rasters whose cells took these values. This operation was performed in ArcGIS 10.5 software using the Lookup tool in the Spatial Analyst extension. For the derivation of the Flood Potential Index (IPI) values on the Danube Delta, the new rasters were included in the following equation that was implemented in the Raster Calculator tool in ArcGIS 10.5:

$$\text{PIAHP} = 0.288\times [\text{Slope}] + 0.239\times [\textit{Elevation}] + 0.177\times [\textit{Distance from river}] + 0.124\times [\textit{Land use}] + 0.068\times [\textit{Altitude above channel}] + 0.049^{*} [\text{Distance from water bodies}] + 0.038\times [\textit{Lithology}] + 0.016\times [\textit{Hydrological Soil Groups}] \quad (11)$$

Once the weights for each factor and factor class were determined, the FPI values were derived by applying (11). It should be mentioned that the surfaces of the lakes were excluded from this analysis because there is always water in them. The FPI values were grouped into four classes by using the Natural Breaks classification method (Figure 6a). The very low values of FPI are spread over 12.17% of the total study area (Figure 7).

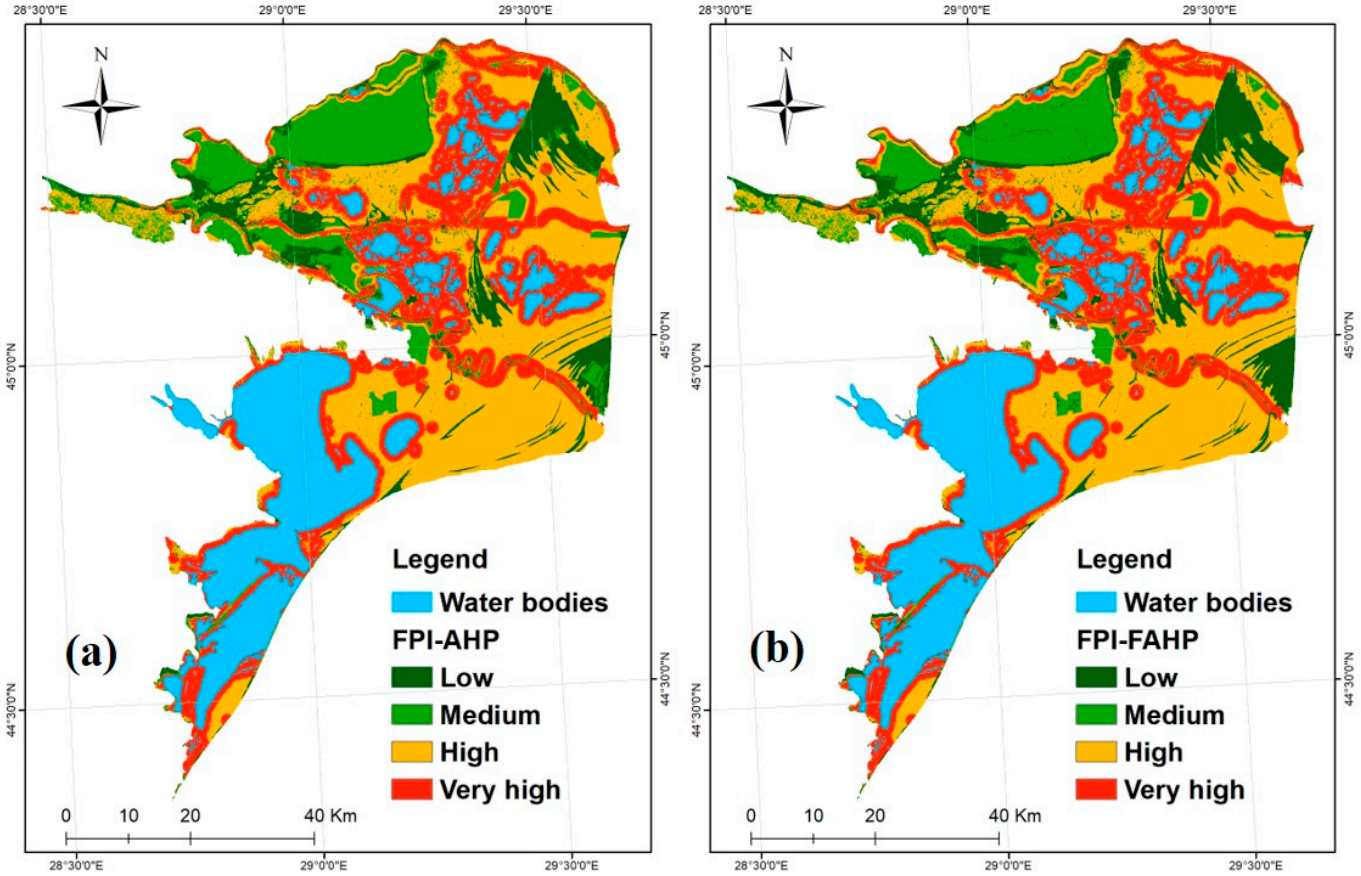


**Figure 6.** Flood Potential Index (FPI). (**a**) AHP, (**b**) FAHP.

In these areas, the potential for flooding is reduced due to the higher altitudes, the presence of forested areas, and the greater distance from the Danube arms and canals. The average values of the FPI occupy 16.36% of the study area. The next class is the one corresponding to the high potential for flooding. This is distributed on about 39.66% of the total (Figure 7) and appears in the areas delimited by the canals in the study area and the Danube arms. Areas with very high values of the FPI cover approximately 31.81% of the surface of the study area. These surfaces are generally present in areas with low altitudes of less than 1 m, near the Danube arms and canals. They are generally arranged on soil with a low degree of permeability above which the lack of forest cover is noticeable.

### *5.2. Fuzzy-AHP Method*

A pairwise comparison matrix was created in Microsoft Excel to determine flood susceptibility using the Fuzzy-AHP method. We compared the importance of all eight flash flood predictors in this matrix (Table 3) based on their association with flood genesis.

Calculated using the comparison matrix, these synthesis values were derived using the equation below:

$$\left[\sum_{k=1}^{n}\sum_{j=1}^{n} a'_{kj}\right]^{-1} = (78.39\ 107.85\ 142.12)^{-1} = (0.007\ 0.0093\ 0.012) \quad (12)$$

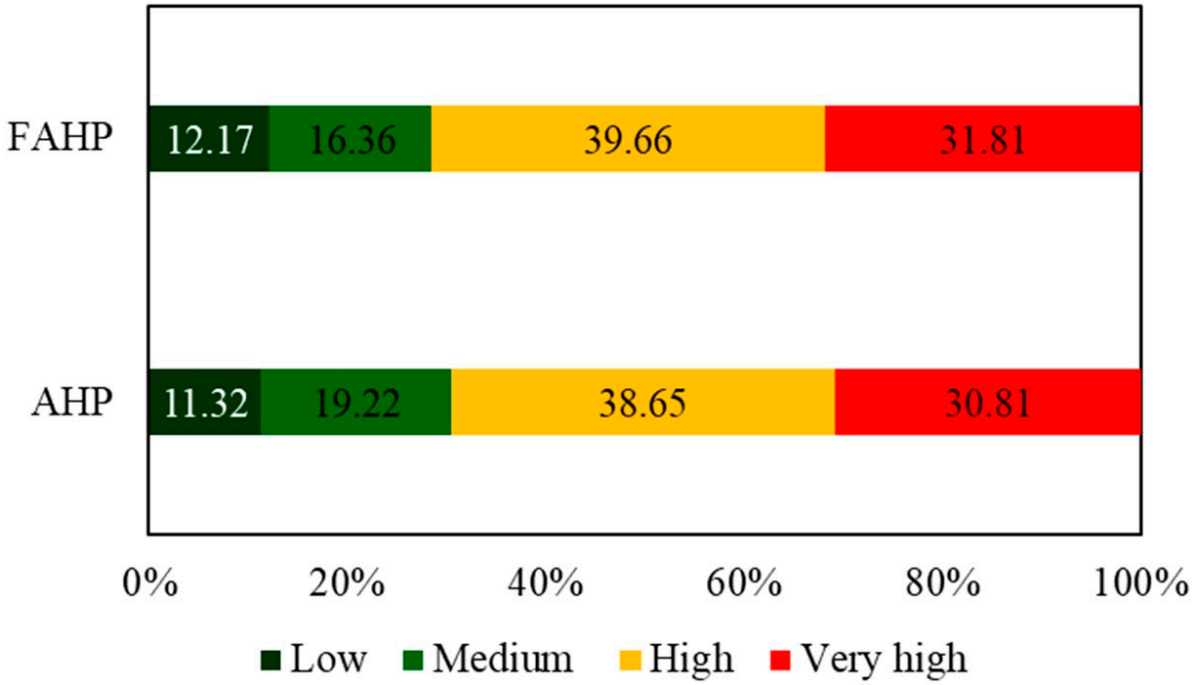


**Figure 7.** Weights of flood potential index (FPI) classes.

**Table 3.** FAHP evaluation matrix.

| | 1 | 2 | 3 | 4 | 5 | 6 | 7 | 8 |
|---|---|---|---|---|---|---|---|---|
| Slope (1) | | | | | | | | |
| $l_1$ | 1 | 1 | 2 | 3 | 3 | 4 | 4 | 5 |
| $m_1$ | 1 | 2 | 3 | 4 | 4 | 5 | 5 | 6 |
| $u_1$ | 1 | 3 | 4 | 5 | 5 | 6 | 6 | 7 |
| Elevation (2) | | | | | | | | |
| $l_2$ | 1/3 | 1 | 1 | 2 | 3 | 4 | 4 | 4 |
| $m_2$ | 1/2 | 1 | 2 | 3 | 4 | 5 | 5 | 5 |
| $u_2$ | 1 | 1 | 3 | 4 | 5 | 6 | 6 | 6 |
| Distance from river (3) | | | | | | | | |
| $l_3$ | 1/4 | 1/3 | 1 | 1 | 2 | 2 | 2 | 3 |
| $m_3$ | 1/3 | 1/2 | 1 | 2 | 3 | 3 | 3 | 4 |
| $u_3$ | 1/2 | 1 | 1 | 3 | 4 | 4 | 4 | 5 |
| Land use (4) | | | | | | | | |
| $l_4$ | 1/5 | 1/4 | 1/3 | 1 | 1 | 1 | 1 | 2 |
| $m_4$ | 1/4 | 1/3 | 1/2 | 1 | 2 | 2 | 2 | 3 |
| $u_4$ | 1/3 | 1/2 | 1 | 1 | 3 | 3 | 3 | 4 |
| Altitude above channel (5) | | | | | | | | |
| $l_5$ | 1/5 | 1/4 | 1/3 | 1/3 | 1 | 1 | 1 | 2 |
| $m_5$ | 1/4 | 1/3 | 1/2 | 1/2 | 1 | 2 | 2 | 3 |
| $u_5$ | 1/3 | 1/2 | 1 | 1 | 1 | 3 | 3 | 4 |
| Distance from water bodies (6) | | | | | | | | |
| $l_6$ | 1/6 | 1/5 | 1/4 | 1/3 | 1/3 | 1 | 1 | 1 |
| $m_6$ | 1/5 | 1/4 | 1/3 | 1/2 | 1/2 | 1 | 1 | 2 |
| $u_6$ | 1/4 | 1/3 | 1/2 | 1 | 1 | 1 | 1 | 3 |
| Lithology (7) | | | | | | | | |
| $l_7$ | 1/6 | 1/5 | 1/4 | 1/3 | 1/3 | 1 | 1 | 1 |
| $m_7$ | 1/5 | 1/4 | 1/3 | 1/2 | 1/2 | 1 | 1 | 2 |
| $u_7$ | 1/4 | 1/3 | 1/2 | 1 | 1 | 1 | 1 | 3 |
| Hydrological Soil Groups (8) | | | | | | | | |
| $l_8$ | 1/7 | 1/6 | 1/5 | 1/4 | 1/4 | 1/3 | 1/3 | 1 |
| $m_8$ | 1/6 | 1/5 | 1/4 | 1/3 | 1/3 | 1/2 | 1/2 | 1 |
| $u_8$ | 1/5 | 1/4 | 1/3 | 1/2 | 1/2 | 1 | 1 | 1 |

As a result of these findings, fuzzy numbers were calculated and assigned to each flash flood predictor in order to assign them a relative importance (Table 4).

**Table 4.** The ordinate of the highest intersection point, the degree possibility for TFNs, and the wright's landslide predictors.

| **Slope = 1** | **Elevation = 2** | **Distance from River = 3** |
|---|---|---|
| $V(S1 \geq S2) = 1$ | $V(S2 \geq S1) = 1$ | $V(S3 \geq S1) = 0.51$ |
| $V(S1 \geq S3) = 1$ | $V(S2 \geq S3) = 1$ | $V(S3 \geq S2) = 0.65$ |
| $V(S1 \geq S4) = 1$ | $V(S2 \geq S4) = 1$ | $V(S3 \geq S4) = 1$ |
| $V(S1 \geq S5) = 1$ | $V(S2 \geq S5) = 1$ | $V(S3 \geq S5) = 1$ |
| $V(S1 \geq S6) = 1$ | $V(S2 \geq S6) = 1$ | $V(S3 \geq S6) = 1$ |
| $V(S1 \geq S7) = 1$ | $V(S2 \geq S7) = 1$ | $V(S3 \geq S7) = 1$ |
| $V(S1 \geq S8) = 1$ | $V(S2 \geq S8) = 1$ | $V(S3 \geq S8) = 1$ |
| $\min\{V(S_1 \geq S_k)\} = 1$ | $\min\{V(S_2 \geq S_k)\} = 1$ | $\min\{V(S_3 \geq S_k)\} = 0.51$ |
| Weight = 0.328 | Weight = 0.328 | Weight = 0.166 |
| **Land use = 4** | **Altitude above channel = 5** | **Distance from water bodies = 6** |
| $V(S4 \geq S1) = 0.33$ | $V(S5 \geq S1) = 0.22$ | $V(S6 \geq S1) = 0$ |
| $V(S4 \geq S2) = 0.69$ | $V(S5 \geq S2) = 0.59$ | $V(S6 \geq S2) = 0$ |
| $V(S4 \geq S3) = 1$ | $V(S5 \geq S3) = 0.9$ | $V(S6 \geq S3) = 0.17$ |
| $V(S4 \geq S5) = 1$ | $V(S5 \geq S4) = 1$ | $V(S6 \geq S4) = 0.53$ |
| $V(S4 \geq S6) = 1$ | $V(S5 \geq S6) = 1$ | $V(S6 \geq S5) = 0.63$ |
| $V(S4 \geq S7) = 1$ | $V(S5 \geq S7) = 1$ | $V(S6 \geq S7) = 1$ |
| $V(S4 \geq S8) = 1$ | $V(S5 \geq S8) = 1$ | $V(S6 \geq S8) = 1$ |
| $\min\{V(S_5 \geq S_k)\} = 0.33$ | $\min\{V(S_6 \geq S_k)\} = 0.22$ | $\min\{V(S_7 \geq S_k)\} = 0$ |
| Weight = 0.107 | >Weight = 0.072 | Weight = 0 |
| **Lithology = 7** | **Hydrological Soil Groups = 8** | |
| $V(S7 \geq S1) = 0$ | $V(S8 \geq S1) = 0$ | |
| $V(S7 \geq S2) = 0$ | $V(S8 \geq S2) = 0$ | |
| $V(S7 \geq S3) = 0.17$ | $V(S8 \geq S3) = 0$ | |
| $V(S7 \geq S4) = 0.53$ | $V(S8 \geq S4) = 0.16$ | |
| $V(S7 \geq S5) = 0.63$ | $V(S8 \geq S5) = 0.24$ | |
| $V(S7 \geq S6) = 1$ | $V(S8 \geq S6) = 0.57$ | |
| $V(S7 \geq S8) = 1$ | $V(S8 \geq S7) = 0.57$ | |
| $\min\{V(S_7 \geq S_k)\} = 0$ | $\min\{V(S_8 \geq S_k)\} = 0$ | |
| Weight = 0 | Weight = 0 | |

Each flash flood predictor was then given fuzzy numbers based on these results. The fuzzy number was used as a next step to determine the degree of possibility (Table 4). The following equations were used to determine the weight of each flash flood predictor:

$$w'(a_i) = \{1\ 1\ 0.51\ 0.33\ 0.22\ 0\ 0\ 0\}^{\mathrm{T}} \quad (13)$$

$$w(a_i) = \{0.327\ 0.327\ 0.166\ 0.107\ 0.071\ 0\ 0\ 0\}^{\mathrm{T}} \quad (14)$$

Additionally, the defuzzification process converts TFNs into crunchy weights that are multiplied by AHP values to create $FPI_{FAHP}$ by adding flash flood conditioning factors to them:

$$\begin{aligned} FPI_{FAHP} = {} & 0.328 \times [\textit{Slope}] + 0.328 \times [\textit{Elevation}] + 0.166 \times [\textit{Distance from river}] + \\ & 0.107 \times [\textit{Land use}] + 0.072 \times [\textit{Altitude above channel}] \end{aligned} \quad (15)$$

Equation (15) was implemented in Map Algebra to derive the FPI values. It should be mentioned that the surfaces of the lakes were excluded from this analysis because they always contain water. Like in AHP, the FPI values were grouped into four classes using the Natural Breaks classification method (Figure 6b). The low values of flood susceptibility can be found on 11.32% of the Danube Delta surface (Figure 7). The medium FPI values are spread on 19.22% of the study area, while the next class corresponds to the high potential

for flooding, which is distributed on approximately 38.65% of the study zone. Areas with very high values of the FPI cover approximately 30.81% of the surface of the study area.

## 6. Discussion

Many natural hazards can cause damage, but flooding is among the most prevalent and destructive. As floods become more common throughout the world, they are causing increased losses of life and socio-economic damage to communities and putting significant pressure on them [33]. Considering this massive burden of flooding on human societies, geophysicists, hydrologists, engineers of water resources, geologists, morphologists, as well as a variety of other scientists have taken up the task of studying this phenomenon from many different aspects to mitigate its financial damages and meet its management requirements [34]. They are faced with the vital task of identifying the areas within a watershed to implement a system that can be used to identify those areas that are highly vulnerable to flooding [35]. They use different tools to perform this. Fieldwork is one option that might be preferred, but it is very time-consuming, cost-prohibitive, and hard to conduct. A high-speed alternative to the fieldwork is represented by the computation of flood susceptibility using many flood predictors. Managing flood risk is more manageable with reliable flood susceptibility maps that give land-use managers and government officials essential tools for managing flood risks. In order for a flood to occur, several factors must come together, including those that are outside the river itself, such as factors related to weather, hydrological, geomorphological, geological, land use, and anthropogenic factors, and those that are inside the river, such as hydrological and hydraulic models [36]. There is no precise agreement on which factors should be applied for assessing flood susceptibility, so it is vital to be aware of this. According to Mahmoud et al. [37], it is recommended that more than six factors be used in order to avoid the production of unrepresentative weights dominated by a single factor, which may increase the risk of overrating some of the flood factors. As well as adjusting the number of flood conditioning factors for the local geomorphologic and geologic conditions (to take into account the area's topography and geology, depending on the local conditions), it is essential to take into account the climatic conditions of the area [38]. Although some factors are highly interrelated, each factor contributes more information to the model and enhances the likelihood of realistic results being found. Flood occurrence is strongly correlated with low distances to rivers and the density of rivers, which are both correlated with the lowest distances to rivers [39]. Overbank flooding is more likely to occur in these areas when heavy rainfall over a prolonged period happens [40].

The lithology of the flood plain, the deltas, and the coastal zone strongly correlate with unconsolidated sediments, mainly because these materials underlie the surface of the floodplain, delta, and coastal zone. The present research assigned the highest weight to the slope predictor. This result is in total agreement with the research works carried out by Arora et al. [41], Azareh et al. [42], and Bui et al. [43]. In the case of AHP modeling, all the flood predictors received weights higher than 0, while the calculations carried out in the case of Fuzzy-AHP modeling revealed three flood predictors that received a weight equal to 0. Therefore, these three predictors were not considered in the final computation of flood susceptibility. The very high exposed areas to flood phenomena are located within the zones with the lowest altitude and slopes equal to 0°. Other important factors were the low altitude above the channel, the presence of the river network's proximity, and the presence of built-up and marsh areas [44]. These findings are in total agreement with the works conducted by Ali et al. [45], Bronstert [46], and Chapi [47].

It should be mentioned that the Danube Delta is a region with a poor precipitation regime, with annual precipitation that does not exceed 450 mm. At the same time, it should be mentioned that the floods that occur in the case of the Danube Delta as a result of floods propagating along the Danube, these being the effect of inseminated precipitation that is recorded on the entire surface of the Danube basin, including here its large tributaries such as: Sava, Drava, Tisa, Morava, etc. Therefore, in the case of the study area within the

present research, neither the local climatic factor, nor its temporal variation, is the most important for the occurrence of floods. This is the main reason for which the climatic factor (precipitation) was not taken into account in the present study. It should be also highlighted the very important role that GIS and Remote Sensing technique have in these types of studies [48]. The radar products are part of Remote Sensing techniques [49] and have a crucial role in tracking the severe weather and in the flood forecasting and warning.

## 7. Conclusions

Two multicriteria decision-making models were used in this research to estimate the flood susceptibility of the Danube Delta from Romania. The study's results showed that slope angle, elevation, and distance from the river were the most important factors in the case of both AHP and Fuzzy-AHP models. Moreover, according to the results of the manuscript, the areas covered by a high and very high flood susceptibility account for around 70% of the Danube Delta.

A significant novelty of the present study is the application of these two models for the first time to estimate the flood susceptibility across the Danube Delta, one of the most important deltaic regions at the European level and worldwide. In the literature, no previous research has approached the subject of flood susceptibility in the Danube Delta. There are several good reasons why these two models have been adopted by other research papers and applied in other areas of study as a result of their very high performance. However, at the same time, as a future direction of research, the study's authors consider that the methodology for estimating the risk of flooding should be incorporated into a broader methodology for estimating the risk of floods as part of a more comprehensive approach to the estimation of these phenomena. Therefore, it is expected that the socio-economic objectives of the area under study will also be considered in future studies. There is also an effort to conduct detailed case studies on floodplains by considering hydraulic modeling and utilizing digital land models with a high spatial resolution, which will enable detailed case studies to be conducted.

**Author Contributions:** Conceptualization, A.C. and R.C.; methodology, R.C., A.B. and S.C.P.; software, R.C. and S.C.P.; validation, A.C., A.B., I.C. and C.Ș.D.; formal analysis, A.C. and R.C.; investigation, R.C.; resources, A.C. and R.C.; data curation, A.B. and C.Ș.D.; writing—original draft preparation, R.C. and I.C.; writing—review and editing, A.C., R.C., I.C. and C.Ș.D.; visualization, A.C. and R.C.; supervision, R.C.; project administration, A.B.; funding acquisition, A.B. All authors have read and agreed to the published version of the manuscript.

**Funding:** This research received no external funding.

**Institutional Review Board Statement:** Not applicable.

**Informed Consent Statement:** Not applicable.

**Data Availability Statement:** Not applicable.

**Conflicts of Interest:** The authors declare no conflict of interest.

## References

1. Alho, P.; Aaltonen, J. Comparing a 1D Hydraulic Model with a 2D Hydraulic Model for the Simulation of Extreme Glacial Outburst Floods. *Hydrol. Process.* **2008**, *22*, 1537–1547. [CrossRef]
2. Zhang, Z.; Luo, C.; Zhao, Z. Application of probabilistic method in maximum tsunami height prediction considering stochastic seabed topography. *Nat. Hazards* **2020**, *104*, 2511–2530. [CrossRef]
3. Quan, Q.; Gao, S.; Shang, Y.; Wang, B. Assessment of the sustainability of Gymnocypris eckloni habitat under river damming in the source region of the Yellow. *Sci. Total Environ.* **2021**, *778*, 146312. [CrossRef] [PubMed]
4. Zhang, K.; Ali, A.; Antonarakis, A.; Moghaddam, M.; Saatchi, S.; Tabatabaeenejad, A.; Chen, R.; Jaruwatanadilok, S.; Cuenca, R.; Crow, T.W.; et al. The sensitivity of North American terrestrial carbon fluxes to spatial and temporal variation in soil moisture: An analysis using radar-derived estimates of root-zone soil moisture. *J. Geophys. Res. Biogeosci.* **2019**, *124*, 3208–3231. [CrossRef]
5. Ahmadlou, M.; Karimi, M.; Alizadeh, S.; Shirzadi, A.; Parvinnejhad, D.; Shahabi, H.; Panahi, M. Flood Susceptibility Assessment Using Integration of Adaptive Network-Based Fuzzy Inference System (ANFIS) and Biogeography-Based Optimization (BBO) and BAT Algorithms (BA). *Geocarto Int.* **2019**, *34*, 1252–1272. [CrossRef]

6. O'Neill, B.C.; Oppenheimer, M.; Warren, R.; Hallegatte, S.; Kopp, R.E.; Pörtner, H.O.; Scholes, R.; Birkmann, J.; Foden, W.; Licker, R. IPCC Reasons for Concern Regarding Climate Change Risks. *Nat. Clim. Chang.* **2017**, *7*, 28–37. [CrossRef]
7. Jain, P.; Coogan, S.C.; Subramanian, S.G.; Crowley, M.; Taylor, S.; Flannigan, M.D. A Review of Machine Learning Applications in Wildfire Science and Management. *Environ. Rev.* **2020**, *28*, 478–505. [CrossRef]
8. Zhang, K.; Wang, S.; Bao, H.; Zhao, X. Characteristics and influencing factors of rainfall-induced landslide and debris flow hazards in Shaanxi Province, China. *Nat. Hazards Earth Syst. Sci.* **2019**, *19*, 93–105. [CrossRef]
9. Zhang, K.; Shalehy, M.H.; Ezaz, G.T.; Chakraborty, A.; Mohib, K.M.; Liu, L. An integrated flood risk assessment approach based on coupled hydrological-hydraulic modeling and bottom-up hazard vulnerability analysis. *Environ. Model Softw.* **2022**, *148*, 105279. [CrossRef]
10. Liu, Y.; Zhang, K.; Li, Z.; Liu, Z.; Wang, J.; Huang, P. A hybrid runoff generation modelling framework based on spatial combination of three runoff generation schemes for semi-humid and semi-arid watersheds. *J. Hydrol.* **2020**, *590*, 125440. [CrossRef]
11. Hong, H.; Tsangaratos, P.; Ilia, I.; Liu, J.; Zhu, A.-X.; Chen, W. Application of Fuzzy Weight of Evidence and Data Mining Techniques in Construction of Flood Susceptibility Map of Poyang County, China. *Sci. Total Environ.* **2018**, *625*, 575–588. [CrossRef] [PubMed]
12. Rateb, A.; Abotalib, A.Z. Inferencing the Land Subsidence in the Nile Delta Using Sentinel-1 Satellites and GPS between 2015 and 2019. *Sci. Total Environ.* **2020**, *729*, 138868. [CrossRef] [PubMed]
13. Wang, S.; Zhang, K.; Chao, L.; Li, D.; Tian, X.; Bao, H.; Chen, G.; Xia, Y. Exploring the utility of radar and satellite-sensed precipitation and their dynamic bias correction for integrated prediction of flood and landslide hazards. *J. Hydrol.* **2021**, *603*, 126964. [CrossRef]
14. Asadi, H.; Shahedi, K.; Jarihani, B.; Sidle, R.C. Rainfall-Runoff Modelling Using Hydrological Connectivity Index and Artificial Neural Network Approach. *Water* **2019**, *11*, 212.
15. Gao, C.; Hao, M.; Chen, J.; Gu, C. Simulation and design of joint distribution of rainfall and tide level in Wuchengxiyu Region, China. *Urban Clim.* **2021**, *40*, 101005. [CrossRef]
16. Zhao, F.; Song, L.; Peng, Z.; Yang, J.; Luan, G.; Chu, C.; Ding, J.; Feng, S.; Jing, Y.; Xie, Z. Night-time light remote sensing mapping: Construction and analysis of ethnic minority development index. *Remote Sens.* **2021**, *13*, 2129. [CrossRef]
17. Kim, Y.; Kimball, J.S.; Zhang, K.; Didan, K.; Velicogna, I.; McDonald, K.C. Attribution of divergent northern vegetation growth responses to lengthening non-frozen seasons using satellite optical-NIR and microwave remote sensing. *Int. J. Remote Sens.* **2014**, *35*, 3700–3721. [CrossRef]
18. Chukwuma, E.; Okonkwo, C.; Ojediran, J.; Anizoba, D.; Ubah, J.; Nwachukwu, C. A GIS Based Flood Vulnerability Modelling of Anambra State Using an Integrated IVFRN-DEMATEL-ANP Model. *Heliyon* **2021**, *7*, e08048. [CrossRef]
19. Chen, W.; Li, W.; Chai, H.; Hou, E.; Li, X.; Ding, X. GIS-Based Landslide Susceptibility Mapping Using Analytical Hierarchy Process (AHP) and Certainty Factor (CF) Models for the Baozhong Region of Baoji City, China. *Environ. Earth Sci.* **2016**, *75*, 63. [CrossRef]
20. Pires, A.; Chang, N.-B.; Martinho, G. An AHP-Based Fuzzy Interval TOPSIS Assessment for Sustainable Expansion of the Solid Waste Management System in Setúbal Peninsula, Portugal. *Resour. Conserv. Recy.* **2011**, *56*, 7–21. [CrossRef]
21. Armaş, I.; Avram, E. Perception of Flood Risk in Danube Delta, Romania. *Nat. Hazards* **2009**, *50*, 269–287. [CrossRef]
22. Zhou, G.; Song, B.; Liang, P.; Xu, J.; Yue, T. Voids Filling of DEM with Multiattention Generative Adversarial Network Model. *Remote Sens.* **2022**, *14*, 1206. [CrossRef]
23. Carey, S.K.; Woo, M. Slope Runoff Processes and Flow Generation in a Subarctic, Subalpine Catchment. *J. Hydrol.* **2001**, *253*, 110–129. [CrossRef]
24. Costache, R. Flood Susceptibility Assessment by Using Bivariate Statistics and Machine Learning Models-A Useful Tool for Flood Risk Management. *Water Resour. Manag.* **2019**, *33*, 3239–3256. [CrossRef]
25. Costache, R.; Bao Pham, Q.; Corodescu-Roșca, E.; Cîmpianu, C.; Hong, H.; Thi Thuy Linh, N.; Ming Fai, C.; Najah Ahmed, A.; Vojtek, M.; Muhammed Pandhiani, S. Using GIS, Remote Sensing, and Machine Learning to Highlight the Correlation between the Land-Use/Land-Cover Changes and Flash-Flood Potential. *Remote Sens.* **2020**, *12*, 1422. [CrossRef]
26. Prăvălie, R.; Costache, R. The Vulnerability of the Territorial-Administrative Units to the Hydrological Phenomena of Risk (Flash-Floods). Case Study: The Subcarpathian Sector of Buzău Catchment. *An. Univ. Oradea–Ser. Geogr.* **2013**, *23*, 91–98.
27. Dong, J.; Deng, R.; Quanying, Z.; Cai, J.; Ding, Y.; Li, M. Research on recognition of gas saturation in sandstone reservoir based on capture mode. *Appl. Radiat. Isot.* **2021**, *178*, 109939. [CrossRef]
28. Fan, C.; Li, H.; Qin, Q.; He, S.; Zhong, C. Geological conditions and exploration potential of shale gas reservoir in Wufeng and Longmaxi Formation of southeastern Sichuan Basin, China. *J. Pet. Sci. Eng.* **2020**, *191*, 107138. [CrossRef]
29. Xie, W.; Li, X.; Jian, W.; Yang, Y.; Liu, H.; Robledo, L.F.; Nie, W. A novel hybrid method for landslide susceptibility mapping-based geodetector and machine learning cluster: A case of Xiaojin county, China. *ISPRS Int. J. Geo-Inf.* **2021**, *10*, 93. [CrossRef]
30. Agarwal, E.; Agarwal, R.; Garg, R.; Garg, P. Delineation of Groundwater Potential Zone: An AHP/ANP Approach. *J. Earth Syst. Sci.* **2013**, *122*, 887–898. [CrossRef]
31. Costache, R.; Ali, S.A.; Parvin, F.; Pham, Q.B.; Arabameri, A.; Nguyen, H.; Crăciun, A.; Anh, D.T. Detection of Areas Prone to Flood-Induced Landslides Risk Using Certainty Factor and Its Hybridization with FAHP, XGBoost and Deep Learning Neural Network. *Geocarto Int.* **2021**, 1–36. [CrossRef]

32. Gigović, L.; Pamučar, D.; Bajić, Z.; Drobnjak, S. Application of GIS-Interval Rough AHP Methodology for Flood Hazard Mapping in Urban Areas. *Water* **2017**, *9*, 360. [CrossRef]
33. Cao, Y.; Jia, H.; Xiong, J.; Cheng, W.; Li, K.; Pang, Q.; Yong, Z. Flash Flood Susceptibility Assessment Based on Geodetector, Certainty Factor, and Logistic Regression Analyses in Fujian Province, China. *ISPRS Int. J. Geo-Inf.* **2020**, *9*, 748. [CrossRef]
34. Anquetin, S.; Braud, I.; Vannier, O.; Viallet, P.; Boudevillain, B.; Creutin, J.-D.; Manus, C. Sensitivity of the Hydrological Response to the Variability of Rainfall Fields and Soils for the Gard 2002 Flash-Flood Event. *J. Hydrol.* **2010**, *394*, 134–147. [CrossRef]
35. Lee, G.; Jun, K.; Chung, E.-S. Group Decision-Making Approach for Flood Vulnerability Identification Using the Fuzzy VIKOR Method. *Nat. Hazards Earth Syst. Sci.* **2015**, *15*, 863–874. [CrossRef]
36. Sattar, A.; Bonakdari, H.; Gharabaghi, B.; Radecki-Pawlik, A. Hydraulic Modeling and Evaluation Equations for the Incipient Motion of Sandbags for Levee Breach Closure Operations. *Water* **2019**, *11*, 279. [CrossRef]
37. Mahmoud, S.H.; Gan, T.Y. Multi-Criteria Approach to Develop Flood Susceptibility Maps in Arid Regions of Middle East. *J. Clean. Prod.* **2018**, *196*, 216–229. [CrossRef]
38. Xie, W.; Nie, W.; Saffari, P.; Robledo, L.F.; Descote, P.Y.; Jian, W. Landslide hazard assessment based on Bayesian optimization–support vector machine in Nanping City, China. *Nat. Hazards* **2021**, *109*, 931–948. [CrossRef]
39. Costache, R.; Ţîncu, R.; Elkhrachy, I.; Pham, Q.B.; Popa, M.C.; Diaconu, D.C.; Avand, M.; Costache, I.; Arabameri, A.; Bui, D.T. New Neural Fuzzy-Based Machine Learning Ensemble for Enhancing the Prediction Accuracy of Flood Susceptibility Mapping. *Hydrol. Sci. J.* **2020**, *65*, 2816–2837. [CrossRef]
40. Chen, Z.; Liu, Z.; Yin, L.; Zheng, W. Statistical analysis of regional air temperature characteristics before and after dam construction. *Urban Clim.* **2022**, *41*, 101085. [CrossRef]
41. Arora, A.; Pandey, M.; Siddiqui, M.A.; Hong, H.; Mishra, V.N. Spatial Flood Susceptibility Prediction in Middle Ganga Plain: Comparison of Frequency Ratio and Shannon's Entropy Models. *Geocarto Int.* **2019**, *36*, 1–32. [CrossRef]
42. Azareh, A.; Rafiei Sardooi, E.; Choubin, B.; Barkhori, S.; Shahdadi, A.; Adamowski, J.; Shamshirband, S. Incorporating Multi-Criteria Decision-Making and Fuzzy-Value Functions for Flood Susceptibility Assessment. *Geocarto Int.* **2019**, *36*, 1–21. [CrossRef]
43. Bui, D.T.; Tsangaratos, P.; Ngo, P.-T.T.; Pham, T.D.; Pham, B.T. Flash Flood Susceptibility Modeling Using an Optimized Fuzzy Rule Based Feature Selection Technique and Tree Based Ensemble Methods. *Sci. Total Environ.* **2019**, *668*, 1038–1054. [CrossRef] [PubMed]
44. Huang, Y.; Bárdossy, A.; Zhang, K. Sensitivity of hydrological models to temporal and spatial resolutions of rainfall data. *Hydrol. Earth Syst. Sci.* **2019**, *23*, 2647–2663. [CrossRef]
45. Ali, S.A.; Parvin, F.; Pham, Q.B.; Vojtek, M.; Vojteková, J.; Costache, R.; Linh, N.T.T.; Nguyen, H.Q.; Ahmad, A.; Ghorbani, M.A. GIS-Based Comparative Assessment of Flood Susceptibility Mapping Using Hybrid Multi-Criteria Decision-Making Approach, Naïve Bayes Tree, Bivariate Statistics and Logistic Regression: A Case of Topľa Basin, Slovakia. *Ecol. Indic.* **2020**, *117*, 106620. [CrossRef]
46. Bronstert, A. Floods and Climate Change: Interactions and Impacts. *Risk Anal.* **2003**, *23*, 545–557. [CrossRef]
47. Chapi, K.; Singh, V.P.; Shirzadi, A.; Shahabi, H.; Bui, D.T.; Pham, B.T.; Khosravi, K. A Novel Hybrid Artificial Intelligence Approach for Flood Susceptibility Assessment. *Environ. Model. Softw.* **2017**, *95*, 229–245. [CrossRef]
48. Yin, L.; Wang, L.; Keim, B.D.; Konsoer, K.; Zheng, W. Wavelet analysis of dam injection and discharge in three gorges dam and reservoir with precipitation and river discharge. *Water* **2022**, *14*, 567. [CrossRef]
49. Yan, J.; Jiao, H.; Pu, W.; Shi, C.; Dai, J.; Liu, H. Radar Sensor Network Resource Allocation for Fused Target Tracking: A Brief Review. *Inf. Fusion* **2022**, *87–88*, 105–115. [CrossRef]